Side-NSM composite technique for flexural strengthening of RC beams

Md. Akter Hosen[1,2], Mohd Zamin Jumaat[*1], A. B. M. Saiful Islam[3], Md. Abdus Salam[2] and Kim Hung Mo[1]

[1]*Department of Civil Engineering, Faculty of Engineering, University of Malaya, 50603, Kuala Lumpur, Malaysia*
[2]*Department of Civil Engineering, Dhaka University of Engineering & Technology (DUET), Gazipur-1700, Bangladesh*
[3]*Department of Construction Engineering, College of Engineering, University of Dammam, 31451 Dammam, Saudi Arabia*

Abstract. Reinforced concrete (RC) infrastructures often require strengthening due to error in design, degradation of materials properties after prolong utilization and increases load carrying capacity persuaded by new use of the structures. For this purpose, a newly proposed Side Near Surface Mounted (SNSM) composite technique was used for flexural strengthening of RC beam specimens. Analytical and non-linear finite element modeling (FEM) using ABAQUS were performed to predict the flexural performance of RC specimens strengthened with S-NSM using steel bars as a strengthening reinforcement. RC beams with various SNSM reinforcement ratios were tested for flexural performance using four-point bending under monotonic loading condition. Results showed significantly increase the yield and ultimate strengths up to 140% and 144% respectively and improved failure modes. The flexural response, such as failure load, mode of failure, yield load, ultimate load, deflection, strain, cracks characteristic and ductility of the beams were compared with those predicted results. The strengthened RC beam specimens showed good agreement of predicted flexural behavior with the experimental outcomes.

Keywords: SNSM composite; numerical simulation; analytical model; ductility; strengthening

1. Introduction

Existing civil engineering structures are struggling to cope with updated code requirements, functional alterations and the need to extend service life (Toutanji *et al.* 2006). Strengthening is inevitably a good choice in terms of structural efficacy as well as from an economic point of view. Externally Bonded Reinforcement (EBR) 994 (Arduini and Nanni 1997, Hawileh *et al.* 2014, Hildebrand 1994, Sharif *et al.* 1994) and Near Surface Mounted (NSM) (Laura De Lorenzis *et al.* 2000, El-Hacha and Rizkalla 2004, Lorenzis and Nanni 2001) strengthening methods are attracted more awareness of the international Civil engineering community. The EBR technique (Bossio *et al.* 2015, Martinelli *et al.* 2014) comprises plates or laminates for strengthening, which bonded to the strengthening members by the glue or epoxy adhesive. The crucial drawback of this technique is premature failure of the strengthened members because of enhanced interfacial shear stresses at the plate ends (Akbarzadeh and Maghsoudi 2010, Rahimi and Hutchinson 2001, Zhou *et al.* 2013). Several finite element studies have been carried out for EBR strengthened members (Park *et al.* 2007, Park and Aboutaha 2005, Zhang *et al.* 2016).

Some researchers have suggested that end anchors to be used to overcome this type of failure (Arduini *et al.* 1997, Hosen *et al.* 2015, Jumaat and Alam 2008). The NSM strengthening approach was also introduced to compensate the drawback of EBR technique. In the NSM system, the strengthening strips or rods are inserted into grooves with epoxy adhesive after cutting the concrete cover (De Lorenzis and Teng 2007). NSM strengthening offers higher levels of strengthening worth, less vulnerable to debonding failure, improves safeguard from mechanical damage, vandalism acts, fire, and aging effects, as well as improves the durability, stress distribution mechanisms and fatigue behavior (Rosenboom and Rizkalla 2006).

Numerous experimental investigations were performed to examine the bond characteristics of NSM bars or strips in concrete using direct pullout tests (Bilotta *et al.* 2011, Galati and De Lorenzis 2009, Novidis *et al.* 2007, Sharaky *et al.* Sharaky *et al.* 2013, Soliman *et al.* 2010) or beam pullout tests (Laura De Lorenzis *et al.* 2002). Tang *et al.* (2006) assessed the flexural performance of NSM strengthened RC beams with glass fiber reinforced polymer (GFRP) bars. The dominant failure modes were debonding, which happened either shear stress or adhesive splitting or rupture. Al-Mahmoud *et al.* (2009) explored the behavior of NSM-carbon fiber reinforced polymer (CFRP) flexural strengthened RC beams imposed by four point bending loads. The failure mode of the beams were debonding by the splitting or peeling-off bars. Al-Mahmoud *et al.* (2010) also, studied the strengthening outward pressure of cantilever beams strengthened by NSM-CFRP bars. The pullout of the rods causes failure when the CFRP rods had larger length compared to the cracked span and the peeling-off was seen when some of the cracks reached the end of the beam. Sharaky *et al.* (2014) tested RC NSM-FRP strengthened beams for evaluating the flexural responses. The beams failed in debonding. NSM double grooves with CFRP failed due to separation of concrete cover and the GFRP revealed splitting of concrete. Hosen *et al.* (2016)

∗Corresponding author
 E-mail: zamin@um.edu.my

Table 1 Test matrix

| Notation | Strengthening of beams | | | Grooves size (mm) | Bonded length of strengthening bars (mm) |
	Materials	Diameter (mm)	No. of bar		
CB	Unstrengthened beam				
S-NSM1		6			
S-NSM2	Steel bars	8	2	$1.5\, d_b \times 1.5\, d_b$	1900
S-NSM3		10			
S-NSM4		12			

*d_b is the strengthening bar diameter

stated that the Side Near-Surface Mounted (SNSM) strengthening with CFRP bars prominently enhances the flexural capacity, energy absorption capacity and crack characteristics.

Nowadays strengthening of RC elements using CFRP materials very expensive. According to (GangaRao *et al.* 2006) the cost of some types of composite materials in 2005 was $30 per pound, whereas the price of structural steel was around $0.50 to $1.00 per pound. Rahal and Rumaih (2011) proved only 7% to 10% improvement in shear capacity of strengthened beams for use of CFRP than steel. Therefore, the application of steel bars as strengthening reinforcement as a more cost-efficient solution.

This study focuses on the SNSM strengthening technique using steel bars to investigate the flexural behavior of RC beams. The cracking behavior, modes of failure and ductility of RC beams based on the experimental load carrying capacity, deflection and strains values have been analyzed and assessed. Analytical models as well as 3D non-linear finite element models have been developed to predict the flexural responses of RC SNSM-steel composite beams and duly compared with the behavior in experimental investigations.

2. Experimental context

2.1 Test samples

A total of five medium size RC beams had been considered for investigating the flexural performance. The first specimen was without strengthening, which referred as a control beam (CB) and other specimens were strengthened with SNSM technique using different diameters steel of bars. Table 1 presented test matrix for the experimental programme.

2.2 Specimens geometry

The reinforcement detailing of the beams are presented in Fig. 1. In according the ACI code (Committee 2011b) beam specimens were designed as under reinforced. The beam dimensions were 125 mm width, 250 mm height and 2300 mm length with effective span of 2000 mm. The steel bars of 6 mm, 10 mm and 12 mm diameter were used to fabricate the casing of beam specimens. The beams reinforced with 2-12 mm deformed steel bars of grade 500 MPa as a tension reinforcement, which 90° bent at ends for
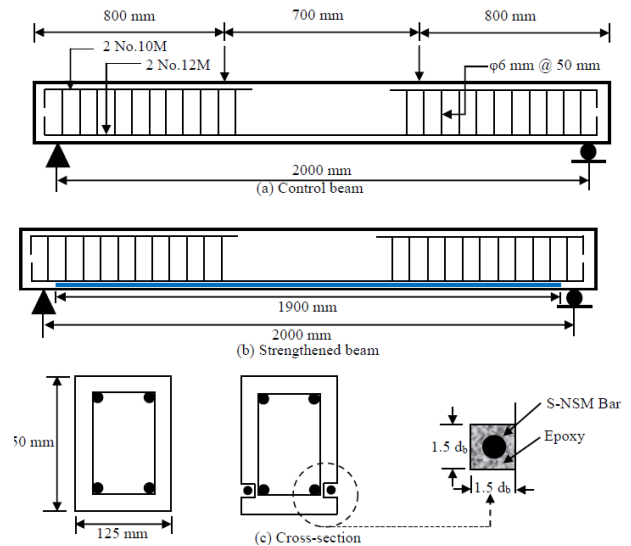

Fig. 1 Detailing of the beam specimens

achieve the anchorage criteria. Top 2-10 mm deformed steel bars of grade 500 MPa used in zone of the shear span. The 6 mm plain bars (250 MPa grade) were used as stirrup which were distributed along its span length (Fig. 1).

2.3 Materials

Ordinary Portland cement was used for casting all the beam specimens while coarse and fine aggregates were crushed granite and manufactured sand respectively. The corresponding maximum size of fine and coarse aggregate was 4.75 mm and 20 mm. For mixing and curing of the concrete potable tap water was used. The concrete had mean compressive strength of 40 MPa and the grade of the SNSM strengthening reinforcement was 500 MPa. The modulus of elasticity of steel reinforcing bars were 200 GPa. Sikadur® 30 epoxy adhesive was used for the bond between the strengthening SNSM-steel and concrete substrate.

2.4 Strengthening schemes

In this method, the strengthening SNSM reinforcement were installed by cutting grooves into the concrete cover from the 25 mm above the beam's tension face in the longitudinal direction at both sides. High pressure air jet and wire brush were used for groove cleaning. Finally, acetone utilized was cleaned the strengthening bars and grooves to eliminate any probable dirt. The groove half-filled using adhesive and a strengthening bar was positioned into the groove and pushed casually. This light forced the flow of epoxy around the SNSM strengthening bar and further adhesive was used to fill up the groove and leveling the surface.

2.5 Instrumentations and testing procedure

The deflection at midspan to measure by vertical linear variable differential transducer (LVDT). For record the strain values, 2-5 mm strain gauges were fixed on the

Table 2 The beams test result summary

Beam ID	P_{cr}		P_y		K_e		P_u		Δ_{max}	Failure mode
	(kN)	(%)	(kN)	(%)	(kN/m)	(%)	(kN)	(%)	(mm)	
CB	15.75	-	70.00	-	6622.52	-	74.37	-	33.61	FL
S-NSM1	27.00	71.43	90.00	28.57	8955.22	35.22	100.00	34.46	41.74	FL
S-NSM2	34.70	120.32	100.00	42.86	9033.42	36.40	108.71	46.17	47.05	FL
S-NSM3	35.00	122.22	125.00	78.57	10245.90	54.71	130.93	76.05	38.56	FL
S-NSM4	50.00	217.46	140.0	100.00	13658.54	106.24	143.57	93.05	35.98	PL

P_{cr} = first cracking load; %P_{cr} = percentile enhance of first cracking load; P_y = yield load; %P_y = percentile enhance of yield load; K_e = effective pre-yield stiffness; %K_e = percentile increase in effective pre-yield stiffness; P_u = ultimate load; %P_u = percentile increase of ultimate load; Δ_{max} = midspan deflection at failure load; FL= flexural failure, PL = peeling-off failure
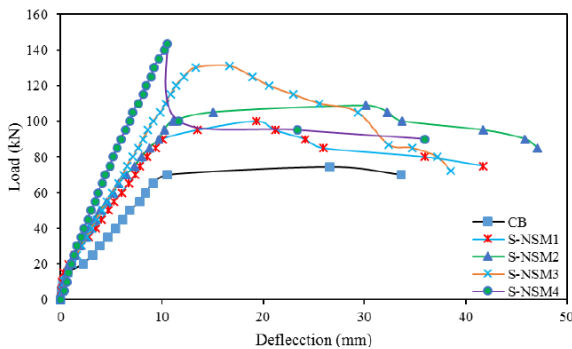

Fig. 2 The deflection behavior of specimens

internal tension bars and the midspan of the SNSM-steel bars, and 30 mm gauge was attached on the extreme surface of the beam respectively. Instron Universal Testing Machine was used for testing of the beams under four point bending at heavy structure laboratory. The load and displacement control was applied for perform the test of the specimens. The rate for load control was 5 kN/min and for displacement control it was 1.5 mm/min. Data was documented at 10 s intervals in TDS-530 data logger and a crack measuring microscope was utilized for crack widths measurement during test.

3. Test results and discussion

The leading features reflected in the investigations are cracking load and crack width, compressive and tensile strain of concrete and steel reinforcement, yield and ultimate load, failure modes and ductility. The summarized test results are demonstrated in Table 2.

3.1 Flexural performance and load-deflection behavior

The Fig. 2 shows the load-midspan deflection curves for all the tested beams. The curves shows tri-linear characteristics, i.e., precracking, cracking and postcracking
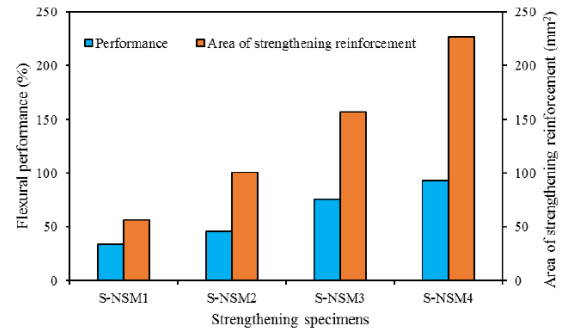

Fig. 3 The effect of strengthening reinforcement

phases except S-NSM4. In the precracking phase, the strengthened beams exhibited linear elastic behavior and the SNSM-steel bars remarkably influenced the beam stiffness due to the side bonded adhesive and bars delay to occurring the cracks. In the cracking phase, the SNSM-steel improved the stiffness and yield load of the specimens. And, final phase, the deflection increased at a higher rate than the load increased compared with the previous phases due to reduce stiffness after reached the ultimate load.

The effective pre-yield stiffness increased by 35.22%, 36.40% 54.71% and 106.24% for S-NSM1, S-NSM2, S-NSM3 and S-NSM4 respectively. In contrast, beam strengthened with NSM steel bars increased the pre-yielding stiffness by a maximum of 60.10% (Almusallam *et al.* 2013). Therefore, new SNSM strengthening remarkably enhanced the pre-yield stiffness and found to be more effective than the conventional NSM strengthening technique due to delay the first crack by this technique.

Fig. 3 shows the strengthened with larger amount (226 mm^2) of SNSM reinforcement improved the flexural performance by 170% compared with the similar beam strengthened with smaller SNSM reinforcement (57 mm^2). The relatively low flexural performance of beams with smaller amount of SNSM reinforcement possibly assigned to their failure modes. The failure took place by concrete crushing at the section's top surface followed by the tension reinforcement (strengthening and main steel bars) yielding except S-NSM4 due to stress transfer from the reinforcements to concrete.

3.2 Mode of failure

The unstrengthened specimens failed by main steel bars' yielding followed by concrete crushing (Fig. 4). The flexural failure occurred by the spreading of a vertical crack, which very close to the beam's midspan. The failure modes of strengthened beams were observed very adjacent to each other and failed by flexure (except S-NSM4 specimens). In this failure mode, a flexural fine crack was developed at midspan and steadily circulated towards the specimen neutral axis. The concrete crushing initiated at the beam's top surface after yielding of main reinforcing steel and the SNSM reinforcement through the formation of concrete wedge and concluding failure arisen by the rupture of SNSM reinforcement (Fig. 4(b)-4(d)). However, the S-NSM4 specimen failed through the peeling off of SNSM bars (Fig. 4(e)) because of yielding of the main reinforcing
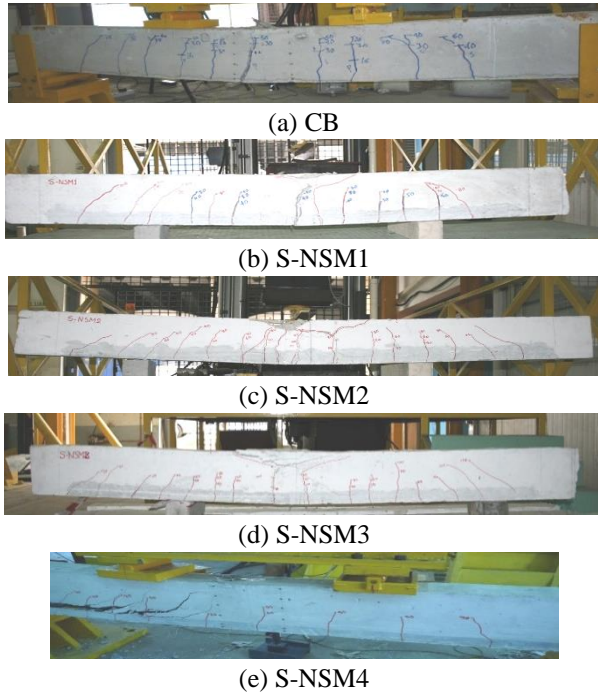
(a) CB

(b) S-NSM1

(c) S-NSM2

(d) S-NSM3

(e) S-NSM4

Fig. 4 Failure modes of beams

Table 3 Ductility and strength index of the beams

Beam ID	Deflection ductility			Energy ductility			Strength index μ_M
	Δ_y (mm)	Δ_u (mm)	μ_d	E_y (kN-mm)	E_u (kN-mm)	μ_E	
CB	10.57	26.56	2.51	412.70	1661.25	4.02	1.06
S-NSM1	10.05	19.35	1.93	522.28	1371.05	2.63	1.11
S-NSM2	11.07	30.15	2.72	660.61	2706.20	4.09	1.08
S-NSM3	12.20	16.67	1.37	844.51	1379.55	1.63	1.05
S-NSM4	10.25	10.50	1.02	781.85	812.48	1.03	1.03

Deflection ductility index, $\mu_d = \Delta_u/\Delta_y$; energy ductility index, $\mu_E = E_u/E_y$; strength index, $\mu_M = M_{max}/M_y$
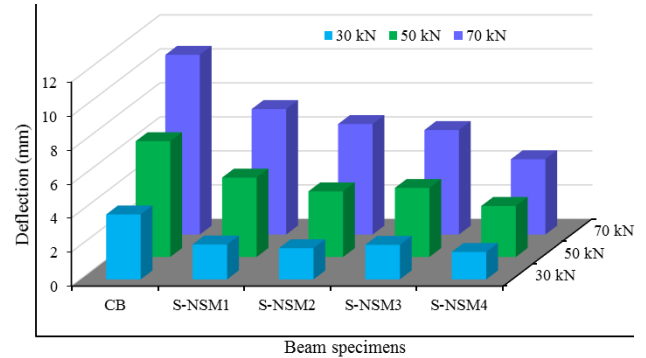

Fig. 5 Decreased deflection and compressive strain due to S-NSM strengthening

steel, the shear cracks were commenced at the SNSM bars' end and the crack widths rapidly increased. Once the shear stress exceeded the bond between the epoxy adhesive and adjacent concrete, the SNSM bars accompanied by adhesive peeled off and encouraged premature failure of the beam.

3.3 Ductility analysis

The ductile behavior of the beam specimens are demonstrated in Table 3. Two ductility indices, namely deflection and energy ductility are determined. The deflection ductility index is defined as a ratio of the deflection at ultimate load (Δ_u) to the deflection at yield load (Δ_y) (Ashour *et al.* 2004). The energy ductility index is defined as a ratio of the energy at ultimate state (E_u) to the energy at yield state (E_y) (Oudah and El-Hacha 2012). The strength index is defined as a ratio of the ultimate bending moment to the yield bending moment. The decrease of ductility in the strengthened specimens owing to the upsurge of tension reinforcement ratio (main steel bars and strengthening bars) (Ramana *et al.* 2000). The lowest deflection and energy ductility index was found in S-NSM4 specimens due to prematurely failure. Also, the strength index decreased by 3% for S-NSM4 specimen over the control beam.

3.4 The effectiveness of Side-NSM-steel technique

The deflection decreased due to SNSM strengthening technique applied in RC beams are revealed in Fig. 5(a). The SNSM-steel maximum decreased deflection of about 58%, 56% and 58% at 30 kN, 50 kN and 70 kN loading over the control specimen, owing to increased stiffness of the specimens. The top fiber concrete compressive normal and decrease strain of the specimens due to applied SNSM-steel technique are shown in Fig. 5(b). The strengthened specimens strain maximum reduced of about 71%, 70% and 73% at 30 kN, 50 kN and 70 kN service loading compared to the control specimen.

4. Numerical simulation

4.1 Material constitutive models

The reinforcement (main and strengthening bars) and concrete was used in this analysis. Reliable constitutive models relevant to reinforcement and concrete are accessible in the ABAQUS materials library (Hsuan-Teh Hu *et al.* 2004).

4.1.1 Steel reinforcement (main and strengthening)

The steel reinforcement modulus of elasticity used in the analyses E_s=200 Gpa. The steel reinforcement stress versus strain curve is assumed as an elasto-plastic. The reinforcement is considered as a uniaxial material all over the element section. The influence of bond-slip influence in between steel and concrete is ignored. The appropriately model of constitutive behavior of the reinforcing steel, and the area, position, orientation and spacing of every layer of reinforcement element prerequisites to be specified.

4.1.2 Concrete

The concrete compressive strain ε_o equivalent to the peak stress f'_c is commonly 0.002–0.003, under uniaxial compression. The ACI Committee 318 (Committee 2011a) recommended a demonstrative value and used in this
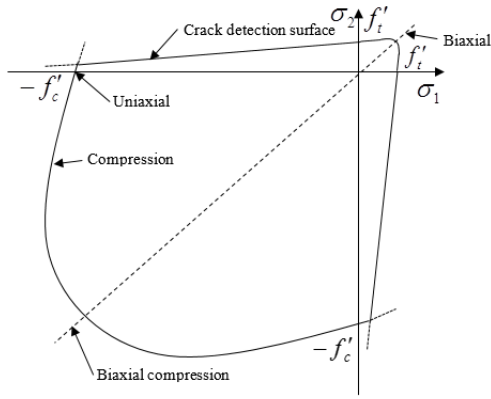
Fig. 6 Plane stress concrete failure surface

analysis is $\varepsilon_o=0.003$. The Poisson's ratio v_c of concrete 0.15–0.22, with an illustrative value of 0.19 or 0.20, under uniaxial compressive stress (Nilson 1982). In this modelling, $v_c=0.20$ is used for concrete. The uniaxial tensile strength of concrete f'_t is taken in this study as (Hu *et al.* 2004).

$$f'_t = 0.33\sqrt{f'_c} \text{ MPa} \tag{1}$$

The concrete modulus of elasticity is vastly interrelated to its compressive strength which might be determined using the following formula (Committee 2011a).

$$E_c = 4700\sqrt{f'_c} \text{ MPa} \tag{2}$$

The concrete failure strengths are observed at different form under multiaxial combinations. Moreover, under multiple stress conditions, the maximum strength envelope to be mostly autonomous of load path (Kupfer *et al.* 1969). A Mohr-Coulomb genre compression face with a crack detection face is employed to the model of the concrete failure surface as shown in Fig. 6.

The principal stress constituents of concrete are primarily in compressive. An elastic-plastic theory and an isotropic hardening principle are employed for modeling of concrete.

When cracks occur in the detection surface, then damaged elasticity is applied for model of the cracks (Hibbitt 2007). At the point once plastic deformation occurs, a particular parameter to guide the extension of the surface. The concrete effective stress (σ_c) and strain (ε_c), which achieved subsequent loading paths of the uniaxial stress versus strain curve. A uniaxial The stress-strain relationship (Desayi and Krishnan 1964) has been usually accepted for concrete as per following equations

$$\sigma_c = \frac{E_c \varepsilon_c}{1+(R+R_E-2)\left(\dfrac{\varepsilon_c}{\varepsilon_0}\right)-(2R-1)\left(\dfrac{\varepsilon_c}{\varepsilon_0}\right)^2+R\left(\dfrac{\varepsilon_c}{\varepsilon_0}\right)^3} \tag{3}$$

$$R = \frac{R_E(R_\sigma-1)}{(R_\varepsilon-1)^2} - \frac{1}{R_\varepsilon}, \quad R_E = \frac{E_c}{E_0}, \quad E_0 = \frac{f'_c}{\varepsilon_0} \tag{4}$$

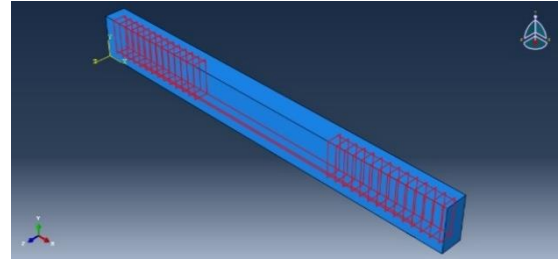And $R_\sigma=4$, $R_\varepsilon=4$ (Hu and Schnobrich 1989)
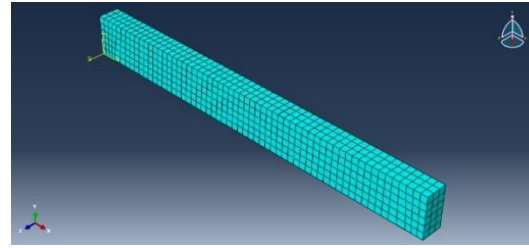

Fig. 7 3D FEM of reinforcements

Fig. 8 3D FE mesh of RC strengthened beams

The micro crack characteristics of concrete is presented by utilizing the smeared model. The reinforced concrete member cracked section still convey more or less tensile stress in the normal direction to the crack, which is named as tension stiffening (Nilson 1982). The elementary descending line was applied to model the concrete tension stiffening in this research. In the postcracking phase, the RC cracked sections carry-over shear forces by the interlocking of aggregate, which is called shear retention. The undamaged concrete shear modulus is G_c, and in the cracked RC section, decreased shear modulus is $\hat{G}$ as follows

$$\hat{G} = \mu G_c \tag{5}$$

$$\mu = 1 - \frac{\varepsilon}{\varepsilon_{max}} \tag{6}$$

The shear retention is perpendicular to the direction of cracks and the parameter μ reduces to zero strains relying on tension stiffening ε and ε_{max}. The ε_{max} is used to be prominent value in ABAQUS, i.e., complete shear retention ($\mu = 1$). In this investigation, the shear retention and tension stiffening values are $\mu = 1$ and $\varepsilon^* = 0.001$ respectively used.

4.1.3 Model geometry

For modelling actual characteristics of experimental tested RC SNSM-steel strengthened beams, the concrete volume was simulated as 3D solid constituents. For this purpose, 8-node trimmed integration solid hexahedron constituents were assumed to the model of concrete and Sikadur® epoxy adhesive follows similar element definition. The 3D algorithms to control the hourglass approaches are used in ABAQUS software. The main reinforcing steel and strengthening bars as well as transverse stirrups were modeled applying 2-node truss elements as shown in Fig. 7. The mesh of SNSM-steel
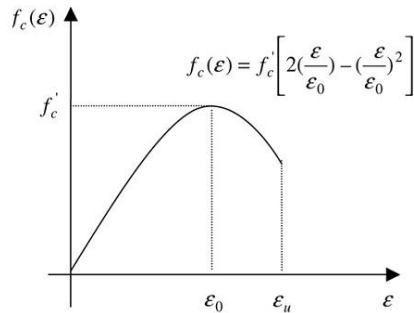
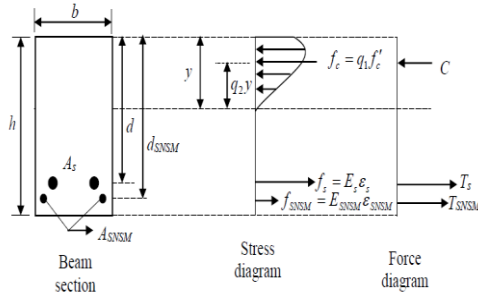Fig. 9 Concrete constitutive model for uniaxial compression

Fig. 10 Stress and forces distribution in SNSM-steel composite section

strengthened composite beams are shown in Fig. 8, which comprises of 1086 19, 824 for solid concrete elements, epoxy elements and truss elements for the reinforcing steel bars respectively and a total elements of 1929. In the FEM analysis, perfect bond between steel reinforcing bars and nearby concrete; SNSM bars and epoxy adhesive and in-between epoxy adhesive and concrete was considered.

5. Analytical model

The prediction model depend on the compatibility of strain as well as sectional analysis of the RC SNSM-steel strengthened beam specimens. The following assumptions were assumed (Badawi and Soudki 2009) in this model:
(i) plane cross-sections continue plane after bending,
(ii) strains in the reinforcing steel and concrete are proportional to the neutral axis (N.A.) depth
(iii) no slip among the concrete and SNSM bars,
(iv) extreme fiber compressive strain in concrete value is 0.003 and
(v) concrete tensile strength is ignored.

5.1 The ultimate load capacity

Generally, the concrete uniaxial compression was used for constitutive model. Assumed, the distribution of strain is linear along the depth of the section and the actual stress-strain relation in concrete extreme fiber is reflected by the predominant branch of the curve as shown in Fig. 9.

The strengthened beams ultimate load were determined (Toutanji *et al.* 2006) by the strain compatibility and force equilibrium requirements as demonstrated in Fig. 10. The iteration procedure was adopted to achieve equilibrium.

From Fig. 10.

$$C = \int_0^{\varepsilon_c} f_c(\varepsilon) \frac{b.y}{\varepsilon_c} d\varepsilon \qquad (7)$$

$$q_1 = \frac{1}{f'_c \varepsilon_c} \int_0^{\varepsilon_c} f_c(\varepsilon) d\varepsilon = \frac{\varepsilon_c}{\varepsilon_o} \left(1 - \frac{1}{3} \frac{\varepsilon_c}{\varepsilon_o} \right) \qquad (8)$$

$$q_2 = \frac{1}{\varepsilon_c} \frac{\int_0^{\varepsilon_c} f_c(\varepsilon)\varepsilon d\varepsilon}{\int_0^{\varepsilon_c} f_c(\varepsilon) d\varepsilon} = \frac{2}{3} \left[\frac{1 - \frac{3}{8}\left(\frac{\varepsilon_c}{\varepsilon_o}\right)}{1 - \frac{1}{3}\left(\frac{\varepsilon_c}{\varepsilon_o}\right)} \right] \qquad (9)$$

Generally, $\varepsilon_o = 0.002$,

$$q_1 = 500\varepsilon_c \left(1 - 166.7\varepsilon_c \right) \qquad (10)$$

$$q_2 = \frac{2 - 375\varepsilon_c}{3 - 500\varepsilon_c} \qquad (11)$$

The bending moment with respect to the concrete (M_c) is conferred by

$$M_c = \int_o^{\varepsilon_c} f_c(\varepsilon) by^2 \frac{\varepsilon}{\varepsilon_c^2} d\varepsilon = q_1 q_2 f'_c by^2 \qquad (12)$$

Therefore, the ultimate bending moment (M_u) is given by

$$M_u = q_1 q_2 f'_c by^2 + A_s f_y(d-y) + A_{SNSM}E_{SNSM}\varepsilon_{SNSM}(d_{SNSM}-y) \quad (13)$$

$$\varepsilon_{SNSM} = \frac{d_{SNSM} - y}{d - y}\varepsilon_S \qquad (14)$$

$$P_u = \frac{2M_u}{L_a} \qquad (15)$$

Where b is beam width, h is beam depth, d is the distance among the concrete extreme fiber and center of gravity (C.G.) of main tensile steel reinforcement, d_{SNSM} is the distance among the concrete extreme fiber and C.G. of SNSM bar, y is neutral axis depth, ε_c is strain of the extreme fiber in concrete, $\varepsilon_s(f_y/E_s)$ is strain in the tensile reinforcing steel, ε_{SNSM} is strain in the SNSM reinforcement, f'_c is concrete compressive strength, A_s is the tension reinforcement area, A_{SNSM} is the SNSM reinforcement area, f_y is the tension reinforcement strength, f_{SNSM} is the SNSM reinforcement strength, C, T_s and T_{SNSM} is the total force in the concrete, tensile reinforcing steel and SNSM reinforcement respectively, L_a is length of the shear span, P_u and M_u is the ultimate load and moment respectively.

5.2 The spacing and width of flexural crack

In according to the Euro-code 2 (EN 2004) maximum flexural crack spacing and width was assessed based on the

neutral axis position of the SNSM-steel composite section.

$$S_{max} = 3.4c + 0.425k_1k_2\frac{\phi}{\rho_{eff}} \qquad (16)$$

$$\rho_{eff} = \frac{A_s + n_{SNSM}A_{SNSM}}{A_{ceff}} \qquad (17)$$

$$A_{ceff} = \min\begin{Bmatrix} 2.5 \times b \times c \\ b \times (h-y)/3 \end{Bmatrix} \qquad (18)$$

$$n_{SNSM} = \frac{E_{SNSM}}{E_c} \qquad (19)$$

$$w_k = S_{max}(\varepsilon_{sm} - \varepsilon_{cm}) \qquad (20)$$

$$\varepsilon_{sm} - \varepsilon_{cm} = \frac{\sigma_s - k_t\frac{f_{ct}}{\rho_{eff}}(1+\alpha_e\rho_{eff})}{E_s} \geq 0.6\frac{\sigma_s}{E_s} \qquad (21)$$

$$\alpha_e = \frac{E_s}{E_c} \qquad (22)$$

Where S_{max} is the flexural crack spacing, c is the concrete cover, k_1 and k_2 is the bond and strain distribution coefficient respectively, ϕ is the main tensile reinforcing steel bar diameter, ρ_{eff} is the effective reinforcing steel ratio, A_{ceff} is area of the concrete in tension, n_{SNSM}, E_{SNSM} and E_s is modular ratio, modulus of elasticity the SNSM bars and modulus of elasticity of the main reinforcing steel reinforcement respectively, w_k is the crack width, ε_{sm} is mean strain in the reinforcement due to tension stiffening effects of concrete, ε_{cm} is mean strain in the concrete among the cracks, σ_s is the tension reinforcement stress, k_t is the duration of loading factor, f_{ct} is the concrete tensile strength and E_c is the modulus of elasticity of concrete.

5.3 Modeling of load-deflection curve

The midspan load-deflection curve for SNSM strengthened beam specimens can be divided into three distinguished linear stages (El-Mihilmy & Tedesco, 2000) as

i) Un-cracked phase ($P < P_{cr}$); ii) Cracking phase ($P_{cr} \leq P \leq P_y$); iii) Postcracking phase ($P_y < P < P_u$)

i) Un-cracked phase: Elastic equations are applied to find out the deflection of the beam specimens utilizing the gross transformed moment of inertia (I_g), which contains the contribution of the SNSM steel bars.

Therefore, deflection of uncrack phase,

$$\Delta_{cr} = \frac{(P_{cr}/2)L_a}{24E_cI_g}(3L^2 - 4L_a^2) \qquad (23)$$

ii) Cracking phase: When applied load P is larger than

the cracking load P_{cr}, the section of the concrete in the locality of the mid-span fine flexural cracks occurred, then the flexural stiffness of the beam reduced. In lower load, where there are no cracks in the concrete, the moment of inertia almost equal to the gross transformed moment of inertia (I_g). Where the tension cracks are located, it equals to the transformed cracked moment of inertia (I_{cr}). The moment of inertia lies between the two values of (I_g) and (I_{cr}). When the tensile forces developed between the concrete and cracks, then the flexural rigidity *EI* refers to tension stiffening. In this period, the effective moment of inertia (I_e) is used because the beam has no longer a constant moment of inertia along of its length. The Eq. (24) determines the effective moment of inertia I_e (Committee 2011b).

$$I_e = I_{cr} + (I_g - I_{cr})\left(\frac{M_{cr}}{M}\right)^3 \qquad (24)$$

Hence, deflection of cracking stage,

$$\Delta_y = \frac{(P_y/2)L_a}{24E_cI_e}(3L^2 - 4L_a^2) \qquad (25)$$

iii) Postcracking phase: In this phase, determine the deflection by curvature along the beam length. To evaluate the curvature by linear interpolation between the first yield of tension reinforcement curvature (ϕ_y) and the ultimate curvature (ϕ_u). The neutral axis (N.A.) depth and ultimate moment can be obtained from the ultimate load capacity section.

$$\phi_u = \frac{\varepsilon_{cu}}{y_u} \qquad (26)$$

$$\phi = \phi_y + \frac{M - M_y}{M_u - M_y}(\phi_u - \phi_y) \qquad (27)$$

$$I_e = \frac{M}{E_c\phi} \qquad (28)$$

Therefore, the deflection of postcracking phase can be estimated from Eq. (25). Where, M is the postcracking any service moment.

6. Comparison of test results

6.1 The ultimate load capacity

Fig. 11 shows a comparison of the experimental ultimate load with the predicted value for the SNSM-steel strengthened beam specimens. The predicted ultimate loads in the figure propose that the variation ranges in between 1% to 6% (except S-NSM4). The S-NSM4 specimen shows more variance among the experimental and predicted values due to peeling off failure. Therefore, the proposed analytical and numerical models are considered to be useful tools in
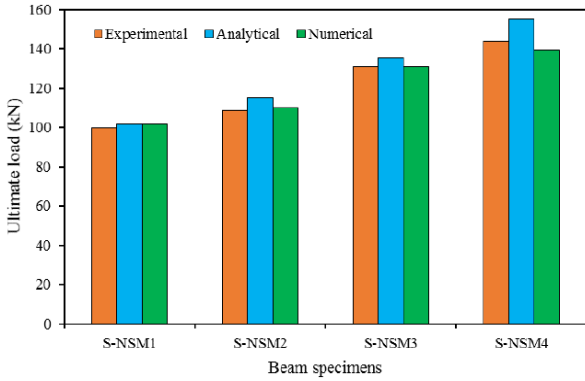
Fig. 11 Predicted and experimental load comparison

predicting the ultimate flexural load carrying capacity of RC beams strengthened by SNSM-steel composite technique.

6.2 The spacing and width of flexural crack

The analytical predicted flexural crack spacings were 155 mm, 111 mm, 102 mm, 96 mm and 93 mm for CB, S-NSM1, S-NSM2, S-NSM3 and S-NSM4 beams, respectively while the experimental values were found to be 180 mm, 115 mm, 106 mm, 102 mm and 96 mm for the CB, S-NSM1, S-NSM2, S-NSM3 and S-NSM4 beams, respectively. Therefore, the predicted and experimental values shows very well agreement with maximum difference of 14%.

The predicted maximum crack widths were 0.32 mm, 0.30 mm, 0.27 mm, 0.26 mm and 0.24 mm for the CB, S-NSM1, S-NSM2, S-NSM3 and S-NSM4 beams, respectively while the experimental crack widths were 0.75 mm, 0.42 mm, 0.29 mm and 0.23 mm and 0.20 mm for CB, S-NSM1, S-NSM2, S-NSM3 and S-NSM4 beams, respectively. The discrepancies between the predicted and experimental crack widths could be possibly due to the predicted higher crack spacing.

6.3 The load-deflection curve

The predicted curves of load-deflection behavior was achieved by applying the proposed models and evaluated with the test results (Fig. 12). The consequences confirmed the validity of the models to predict the deflection curve of RC beams strengthened with SNSM steel reinforcement. The relationship between the experimental, analytical and numerical results of the strengthened beams are within realistic agreement.

6.4 The failure modes

The failure modes of tested beam specimens were discovered from the non-linear FE simulation as shown in Fig. 13. It is shows that predicted failure modes from the FE simulation of the tested beams well matches with the experimental failure modes. It's also observed that, strengthened specimens failed due to rupture of the SNSM reinforcement after the creation of flexural cracks in the
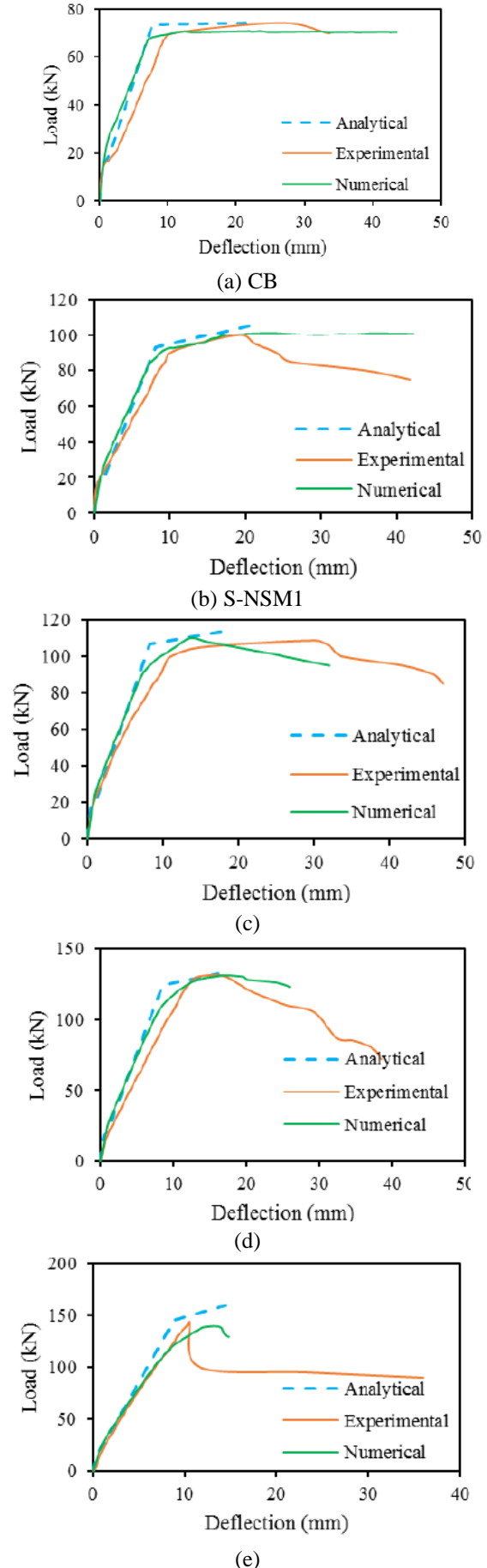

Fig. 12 Prediction of the load-midspan deflection

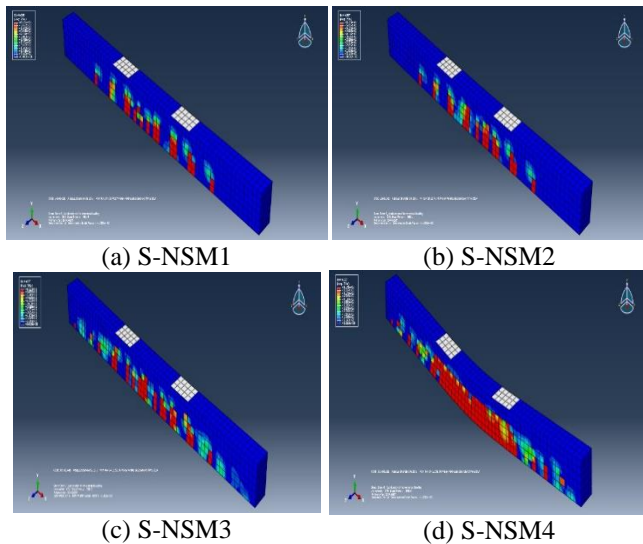(a) S-NSM1   (b) S-NSM2

(c) S-NSM3   (d) S-NSM4

Fig. 13 Failure modes in numerical simulations

constant moment region (except S-NSM4). The S-NSM4 beam failed by peeling off SNSM bars at curtailment location due to occurred shear stress as described in earlier section.

5. Conclusions

Following conclusions can be drawn from the present study:
• The SNSM technique effectively boosted the flexural response and stiffness of RC beams.
• The SNSM-steel bar strengthening (strengthening reinforcement ratios from 0.20 to 0.84%) significantly enhanced first cracking load, yield load and ultimate load by up to 217%, 100% and 93%, respectively than the unstrengthened beam.
• The ultimate flexural capacity of the strengthened RC beams was governed by the tensile rupture of the SNSM bars and full composite behavior of the SNSM reinforcements and its surrounding concrete volume.
• The displacement and energy ductility of flexural strengthened RC beams by SNSM technique was successfully achieved (except S-NSM4).
• Developed 3D finite element model proved its potential ensuring good validation for analyzing the flexural performance of RC beams strengthened with SNSM technique using steel bars.
• The ultimate load and deflection of SNSM-steel strengthened beams could be predicted satisfactorily using the numerical simulations and analytical models.

Acknowledgments

References

ACI (1992), *Standard Practice for Selecting Proportions for Structural Lightweight Concrete (ACI211. 2-91)*.
Akbarzadeh, H. and Maghsoudi, A.A. (2010), "Experimental and analytical investigation of reinforced high strength concrete continuous beams strengthened with fiber reinforced polymer", *Mater. Des.*, **31**(3), 1130-1147.
Al-Mahmoud, F., Castel, A., François, R. and Tourneur, C. (2009), "Strengthening of RC members with near-surface mounted CFRP rods", *Compos. Struct.*, **91**(2), 138-147.
Al-Mahmoud, F., Castel, A., François, R. and Tourneur, C. (2010), "RC beams strengthened with NSM CFRP rods and modeling of peeling-off failure", *Compos. Struct.*, **92**(8), 1920-1930.
Almusallam, T.H., Elsanadedy, H.M., Al-Salloum, Y.A. and Alsayed, S.H. (2013), "Experimental and numerical investigation for the flexural strengthening of RC beams using near-surface mounted steel or GFRP bars", *Constr. Build. Mater.*, **40**, 145-161.
Arduini, M., Di Tommaso, A. and Nanni, A. (1997), "Brittle failure in FRP plate and sheet bonded beams", *ACI Struct. J.*, **94**(4), 363-370.
Arduini, M. and Nanni, A. (1997), "Behavior of precracked RC beams strengthened with carbon FRP sheets", *J. Compos. Constr.*, **1**(2), 63-70.
Ashour, A., El-Refaie, S. and Garrity, S. (2004), "Flexural strengthening of RC continuous beams using CFRP laminates", *Cement Concrete Compos.*, **26**(7), 765-775.
Badawi, M. and Soudki, K. (2009), "Flexural strengthening of RC beams with prestressed NSM CFRP rods-experimental and analytical investigation", *Constr. Build. Mater.*, **23**(10), 3292-3300.
Bilotta, A., Ceroni, F., Di Ludovico, M., Nigro, E., Pecce, M. and Manfredi, G. (2011), "Bond efficiency of EBR and NSM FRP systems for strengthening concrete members", *J. Compos. Constr.*, **15**(5), 757-772.
Bossio, A., Fabbrocino, F., Lignola, G.P., Prota, A. and Manfredi, G. (2015), "Simplified model for strengthening design of beam-column internal joints in reinforced concrete frames", *Polym.*, **7**(9), 1732-1754.
Committee, A. (2011a), *Building Code Requirements for Structural Concrete (318-11) and Commentary-(318R-11)*, American Concrete Institute, Detroit, Michigan, U.S.A.
Committee, A. (2011b), *Building Code Requirements for Structural Concrete (318-11) and Commentary-(318R-11)*, American Concrete Institute, Detroit, Michigan, U.S.A.
De Lorenzis, L., Nanni, A. and La Tegola, A. (2000), "Strengthening of reinforced concrete structures with near surface mounted FRP rods", *Proceedings of the the International Conference on Composite Materials, Advancing with Composites*.
De Lorenzis, L., Rizzo, A. and La Tegola, A. (2002), "A modified pull-out test for bond of near-surface mounted FRP rods in concrete", *Compos. Part B: Eng.*, **33**(8), 589-603.
De Lorenzis, L. and Teng, J. (2007), "Near-surface mounted FRP reinforcement: An emerging technique for strengthening structures", *Compos. Part B: Eng.*, **38**(2), 119-143.
Desayi, P. and Krishnan, S. (1964), "Equation for the stress-strain curve of concrete", *Proceedings of the ACI Journal*.
El-Hacha, R. and Rizkalla, S.H. (2004), "Near-surface-mounted fiber-reinforced polymer reinforcements for flexural strengthening of concrete structures", *ACI Struct. J.*, **101**(5),

717-726.

El-Mihilmy, M.T. and Tedesco, J.W. (2000), "Deflection of reinforced concrete beams strengthened with fiber-reinforced polymer (FRP) plates", *ACI Struct. J.*, **97**(5).

EN, B (2004), *1-1. Eurocode 2: Design of Concrete Structures: Part 1-1: General Rules and Rules for Buildings*, British Standards Institution, London, U.K.

Galati, D. and De Lorenzis, L. (2009), "Effect of construction details on the bond performance of NSM FRP bars in concrete", *Adv. Struct. Eng.*, **12**(5), 683-700.

GangaRao, H.V., Taly, N. and Vijay, P. (2006), *Reinforced Concrete Design with FRP Composites*, CRC Press.

Hawileh, R.A., Rasheed, H.A., Abdalla, J.A. and Al-Tamimi, A.K. (2014), "Behavior of reinforced concrete beams strengthened with externally bonded hybrid fiber reinforced polymer systems", *Mater. Des.*, **53**, 972-982.

Hibbitt, K. (2007), *ABAQUS Version 6. 7: Theory Manual, Users' Manual, Verification Manual and Example Problems Manual: Hibbitt*, Karlson and Sorenson Inc.

Hildebrand, M. (1994), "Non-linear analysis and optimization of adhesively bonded single lap joints between fibre-reinforced plastics and metals", *J. Adhes. Adhes.*, **14**(4), 261-267.

Hosen, M., Jumaat, M.Z., Islam, A., Darain, K. and Rahman, M. (2016), "Flexural performance of reinforced concrete beams strengthened by a new side near-surface mounted technique using carbon fibre-reinforced polymer bars: Experimental and analytical investigation", *Sci. Adv. Mater.*, **8**(4), 726-740.

Hosen, M.A., Jumaat, M.Z. and Islam, A.B.M.S. (2015), "Inclusion of CFRP-epoxy composite for end anchorage in NSM-epoxy strengthened beams", *Adv. Mater. Sci. Eng.*, **5**(10).

Hu, H.T., Lin, F.M. and Jan, Y.Y. (2004), "Nonlinear finite element analysis of reinforced concrete beams strengthened by fiber-reinforced plastics", *Compos. Struct.*, **63**(3), 271-281.

Hu, H.T. and Schnobrich, W.C. (1989), "Constitutive modeling of concrete by using nonassociated plasticity", *J. Mater. Civil Eng.*, **1**(4), 199-216.

Jumaat, M.Z. and Alam, M.A. (2008), "Behaviour of U and L shaped end anchored steel plate strengthened reinforced concrete beams", *Eur. J. Sci. Res.*, **22**(2), 184-196.

Kupfer, H., Hilsdorf, H.K. and Rusch, H. (1969), "Behavior of concrete under biaxial stresses", *Proceedings of the ACI Journal*.

Lorenzis, L.D. and Nanni, A. (2001), "Characterization of FRP rods as near-surface mounted reinforcement", *J. Compos. Constr.*, **5**(2), 114-121.

Martinelli, E., Napoli, A., Nunziata, B. and Realfonzo, R. (2014), "RC beams strengthened with mechanically fastened composites: Experimental results and numerical modeling", *Polym.*, **6**(3), 613-633.

Nilson, A.H. (1982), *State-of-the-Art Report on Finite Element Analysis of Reinforced Concrete*, American Society of Civil Engineers: Task Committee on Finite Element Analysis of Reinforced Concrete Structures of the Structural Division Committee on Concrete and Masonry Structures, New York, U.S.A.

Novidis, D., Pantazopoulou, S. and Tentolouris, E. (2007), "Experimental study of bond of NSM-FRP reinforcement", *Constr. Build. Mater.*, **21**(8), 1760-1770.

Oudah, F. and El-Hacha, R. (2012), "A new ductility model of reinforced concrete beams strengthened using fiber reinforced polymer reinforcement", *Compos. Part B: Eng.*, **43**(8), 3338-3347.

Park, J.G., Lee, K.M., Shin, H.M. and Park, Y.J. (2007), "Nonlinear analysis of RC beams strengthened by externally bonded plates", *Comput. Concrete*, **4**(2), 119-134.

Park, S. and Aboutaha, R. (2005), "Finite element modeling methodologies for FRP strengthened RC members", *Comput.*

Concrete, **2**(5), 389-409.

Rahal, K.N. and Rumaih, H.A. (2011), "Tests on reinforced concrete beams strengthened in shear using near surface mounted CFRP and steel bars", *Eng. Struct.*, **33**(1), 53-62.

Rahimi, H. and Hutchinson, A. (2001), "Concrete beams strengthened with externally bonded FRP plates", *J. Compos. Constr.*, **5**(1), 44-56.

Ramana, V., Kant, T., Morton, S., Dutta, P., Mukherjee, A. and Desai, Y. (2000), "Behavior of CFRPC strengthened reinforced concrete beams with varying degrees of strengthening", *Compos. Part B: Eng.*, **31**(6), 461-470.

Rosenboom, O. and Rizkalla, S. (2006), "Behavior of prestressed concrete strengthened with various CFRP systems subjected to fatigue loading", *J. Compos. Constr.*, **10**(6), 492-502.

Sharaky, I., Torres, L., Baena, M. and Miàs, C. (2013), "An experimental study of different factors affecting the bond of NSM FRP bars in concrete", *Compos. Struct.*, **99**, 350-365.

Sharaky, I., Torres, L., Baena, M. and Vilanova, I. (2013), "Effect of different material and construction details on the bond behaviour of NSM FRP bars in concrete", *Constr. Build. Mater.*, **38**, 890-902.

Sharaky, I., Torres, L., Comas, J. and Barris, C. (2014), "Flexural response of reinforced concrete (RC) beams strengthened with near surface mounted (NSM) fibre reinforced polymer (FRP) bars", *Compos. Struct.*, **109**, 8-22.

Sharif, A., Al-Sulaimani, G., Basunbul, I., Baluch, M. and Ghaleb, B. (1994), "Strengthening of initially loaded reinforced concrete beams using FRP plates", *ACI Struct. J.*, **91**(2), 160-168.

Soliman, S.M., El-Salakawy, E. and Benmokrane, B. (2010), "Bond performance of near-surface-mounted FRP bars", *J. Compos. Constr.*, **15**(1), 103-111.

Tang, W., Balendran, R., Nadeem, A. and Leung, H. (2006), "Flexural strengthening of reinforced lightweight polystyrene aggregate concrete beams with near-surface mounted GFRP bars", *Build. Environ.*, **41**(10), 1381-1393.

Toutanji, H., Zhao, L. and Zhang, Y. (2006), "Flexural behavior of reinforced concrete beams externally strengthened with CFRP sheets bonded with an inorganic matrix", *Eng. Struct.*, **28**(4), 557-566.

Zhang, D., Wang, Q. and Dong, J. (2016), "Simulation study on CFRP strengthened reinforced concrete beam under four-point bending", *Comput. Concrete*, **17**(3), 407-421.

Zhou, Y., Gou, M., Zhang, F., Zhang, S. and Wang, D. (2013), "Reinforced concrete beams strengthened with carbon fiber reinforced polymer by friction hybrid bond technique: Experimental investigation", *Mater. Des.*, **50**, 130-139.

CC